



Published in final edited form as:

J Bone Miner Res. 2019 January ; 34(1): 135–144. doi:10.1002/jbmr.3586.

***miR-219a-5p* Regulates *Rorβ* During Osteoblast Differentiation and in Age-related Bone Loss**

Ruben Aquino-Martinez^{1,*}, Joshua N Farr^{1,2,*}, Megan M Weivoda^{1,2}, Brittany A Negley¹, Jennifer L Onken¹, Brianne S Thicke¹, McKenzie M Fulcer¹, Daniel G Fraser¹, Andre J van Wijnen³, Sundeep Khosla^{1,2}, and David G Monroe^{1,2}

¹Department of Medicine, Division of Endocrinology, Mayo Clinic College of Medicine, Rochester, MN, USA

²Robert and Arlene Kogod Center on Aging, Rochester, MN, USA

³Department of Orthopedic Surgery, Mayo Clinic College of Medicine, Rochester, MN, USA

Abstract

Developing novel approaches to treat skeletal disorders requires an understanding of how critical molecular factors regulate osteoblast differentiation and bone remodeling. We have reported that (1) retinoic acid receptor-related orphan receptor beta (*Rorβ*) is upregulated in bone samples isolated from aged mice and humans in vivo; (2) *Rorβ* expression is inhibited during osteoblastic differentiation in vitro; and (3) genetic deletion of *Rorβ* in mice results in preservation of bone mass during aging. These data establish that *Rorβ* inhibits osteogenesis and that strict control of *Rorβ* expression is essential for bone homeostasis. Because microRNAs (miRNAs) are known to play important roles in the regulation of gene expression in bone, we explored whether a predicted subset of nine miRNAs regulates *Rorβ* expression during both osteoblast differentiation and aging. Mouse osteoblastic cells were differentiated in vitro and assayed for *Rorβ* and miRNA expression. As *Rorβ* levels declined with differentiation, the expression of many of these miRNAs, including *miR-219a-5p*, was increased. We further demonstrated that *miR-219a-5p* was decreased in bone samples from old (24-month) mice, as compared with young (6-month) mice, concomitant with increased *Rorβ* expression. Importantly, we also found that *miR-219a-5p* expression was decreased in aged human bone biopsies compared with young controls, demonstrating that this phenomenon also occurs in aging bone in humans. Inhibition of *miR-219a-5p* in mouse calvarial osteoblasts led to increased *Rorβ* expression and decreased alkaline phosphatase expression and activity, whereas a *miR-219a-5p* mimic decreased *Rorβ* expression and increased osteogenic activity. Finally, we demonstrated that *miR-219a-5p* physically interacts with *Rorβ* mRNA in

Address correspondence to: David G Monroe, Department of Medicine, Division of Endocrinology, Mayo Clinic College of Medicine, Guggenheim 7-11A, 200 First Street SW, Rochester, MN 55905. monroe.david@mayo.edu.

*RA-M and JNF contributed equally to this work.

Authors' roles: DGM conceived and directed the project. DGM, RA, JNF, MMW, AJV, and SK designed the experiments and interpreted the data. DGM, RA, JNF, MMW, BAN, JLO, BST, MMF, and DJF were involved in performing the experiments. DGM wrote and all authors reviewed and approved the final manuscript. DGM accepts responsibility for the integrity of the data analysis and presentation.

Disclosure

All authors state that they have no conflicts of interest.

Additional Supporting Information may be found in the online version of this article.

osteoblasts, defining Ror β as a true molecular target of *miR-219a-5p*. Overall, our findings demonstrate that *miR-219a-5p* is involved in the regulation of Ror β in both mouse and human bone.

Keywords

RorB; MicroRNA; OSTEOLAST; OSTEOPOROSIS; AGING

Introduction

Maintenance of bone mass involves the coordinated activities of bone-forming osteoblasts and bone-resorbing osteoclasts,⁽¹⁾ with important signaling contributions by the matrix-embedded osteocyte.^(2,3) Alterations in the activities among these cell types can lead to either excessive bone resorption or diminished bone formation, resulting in bone loss and the increased risk of fracture.^(4,5) Osteoblast differentiation requires the orchestrated actions of numerous transcription factors (ie, Runx2, osterix) that function to regulate both the formation and maintenance of bone.⁽⁶⁾ Understanding the complexity of the regulation and activity of these and other transcription factors during bone homeostasis is essential to formulate new strategies to combat osteoporotic bone loss and enhance skeletal repair following injury.

The orphan nuclear receptor, Ror β is a transcription factor that has recently been shown to be a negative regulator of bone. Ror β inhibits osteoblast differentiation and Ror β expression increases with age in both mice and human bone-lineage cells,⁽⁷⁻⁹⁾ establishing a reciprocal relation between Ror β expression and osteogenic potential. At the molecular level, Ror β represses both Runx2- and β -catenin-dependent transcriptional activation.^(7,9) Furthermore, global deletion of Ror β in mice results in improved bone mass, microarchitecture, and strength associated with increased bone formation, decreased resorption, and increased activation of the Wnt pathway.⁽⁹⁾ Therefore, the identification and development of novel therapeutic approaches to downregulate Ror β may be a new approach in osteoporosis treatment.

MicroRNAs (miRNAs) comprise a family of small noncoding RNAs (approximately 21 to 22 nucleotides in length) that perform posttranscriptional regulation of gene expression through mRNA degradation and/or translational repression.^(10,11) They exert their gene regulatory function through interaction with short seed sequences usually contained within the 3' untranslated region (UTR) of target genes,⁽¹²⁾ and have been implicated in virtually all essential biological processes, including skeletal development and function.⁽¹³⁻¹⁷⁾ Specific miRNAs have been identified that are associated with osteoporosis, aging, and skeletal fractures.⁽¹⁸⁻²⁰⁾ Because aberrant miRNA expression during either normal or pathological processes has the potential of affecting gene expression and altering a cellular and/or tissue phenotype, it is important to understand how these alterations affect the regulation of key transcription factors in bone, including Ror β .

Ror β expression drastically changes during both osteoblast differentiation and in aging bone in both mice and humans; therefore, we hypothesized that altered miRNA expression

patterns control the expression levels of Ror β , and by extension the cells/tissues in which Ror β functions. Hence, the goal of this study was to specifically identify miRNA(s) that regulate Ror β in osteoblastic cells, as well as in bone samples isolated from mice and humans during aging. Successful identification of these miRNA(s) would provide an alternative therapeutic strategy to downregulate Ror β to promote bone anabolism in the context of age-related bone disorders, such as osteoporosis.

Materials and Methods

Osteoblast cell culture and differentiation

Primary mouse calvarial osteoblasts (CalOBs) were isolated as previously described⁽²¹⁾ and maintained in alpha-minimal essential growth medium (α MEM) supplemented with $1 \times$ antibiotic/antimycotic (ThermoFisher Scientific, Waltham, MA, USA), $1 \times$ Glutamax, and 10% (v/v) fetal bovine serum (GE Healthcare Life Sciences HyClone Laboratories, Logan, UT, USA). For the osteoblast differentiation assays, primary CalOBs were plated at a cell density of 10^4 cells/cm² in 12-well tissue culture plates and allowed to grow to confluence (typically 5 days). At confluence, the media were replaced with osteogenic differentiation medium (growth media supplemented with 50 mg/L ascorbic acid and 10mM β -glycerophosphate; Sigma-Aldrich, St. Louis, MO, USA) and allowed to differentiate for 0, 4, 7, 10, 17, and 24 days ($n = 6$). Osteogenic differentiation media were replaced every 3 days. Cells were lysed in QIAzol reagent (Qiagen, Valencia, CA, USA) for RNA isolation.

qPCR analyses of mRNA and miRNA assays

Total RNA was isolated from either differentiated CalOBs ($n = 6$) or mouse bone homogenates ($n = 10$) using the miRNeasy Mini Kit that included a DNase treatment step (RNase-free DNase Set) using the QIAcube instrument (all reagents from Qiagen). One μ g of total RNA was used to generate cDNA using the High-Capacity cDNA Reverse Transcription Kit (Applied Biosystems, Carlsbad, CA, USA) according to the manufacturer's instructions. qPCR analysis for mRNA expression was performed using the ABI Prism 7900HT Real-Time System instrument (Applied Biosystems) with SYBR Green reagent (Qiagen) as previously described.⁽²²⁾ Data normalization was conducted using multiple endogenous reference genes (*Actb*, *Hprt*, and *Tuba1a*) and threshold calculations are as previously described.⁽²³⁾ The oligonucleotide sequences for the genes measured in this study were designed using the Primer Express program (Applied Biosystems) and are available in Supplemental Table 1.

The miRNA expression data were generated using the same RNA as for the mRNA expression analyses; however, 1 μ g of total RNA was reverse-transcribed using the miScript II RT Kit (Qiagen). The individual miRNA assays used in this study were purchased from Qiagen and used with the miScript SYBR Green PCR Kit (Qiagen) according to the manufacturer's instructions, using the same instrumentation as for the mRNA expression analyses. Data normalization was performed using the *RNU6B* (*U6*) small nucleolar RNA (snRNA).

Bone tissue samples (mouse and human)

All mouse studies were conducted in accordance with NIH guidelines and approved by the Institutional Animal Care and Use Committee at the Mayo Clinic (#A9715–15). Validation and detailed methods of our osteocyte-enriched bone isolation protocol are described extensively elsewhere.⁽²⁴⁾ Briefly, mouse vertebrae isolated from either 6-month-old or 24-month-old male C57BL/6N mice ($n = 10$) were cleaned of associated connective tissue and cut into ~1-mm pieces, which then underwent two sequential 30-min digests in endotoxin-free collagenase (Liberase; Roche Diagnostics GmbH, Mannheim, Germany) and were homogenized in QIAzol (Qiagen) for RNA isolation. The remaining cell fraction has been previously shown to represent a highly enriched population of osteocytes.⁽²⁴⁾ The human bone biopsy samples used in this study were as described in previous publications^(22,25); they were small-needle bone biopsies (isolated from the posterior iliac crest) procured from 10 young premenopausal women (mean age \pm SD, 27 ± 3 years; range 23 to 30 years) and 10 older postmenopausal women (78 ± 5 years; range 72 to 87 years). Postmenopausal status was established by the absence of menses for >1 year and serum follicle stimulate hormone levels >20 IU/L. Extensive exclusion criteria for these patients and the study protocol are as previously described.⁽²²⁾ The RNA from these bone biopsy samples was reanalyzed for miRNA expression.

miR-219a-5p miRNA inhibitor cell model production

Primary CalOBs at approximately 70% confluence were treated overnight with either a negative control miRNA inhibitor lentivirus (Catalog #HLTUD002C) or a custom *miR-219a-5p* miRNA inhibitor lentivirus (MISSION Lenti miRNA Inhibitors; Sigma-Aldrich) at a multiplicity of infection of five virus particles per cell, in the presence of 8- μ g/mL polybrene (Santa Cruz Biotechnology, Santa Cruz, CA, USA) to enhance viral infection. The cells were trypsinized and plated in growth medium supplemented with 1.5- μ g/mL puromycin (ThermoFisher Scientific), which was changed every 3 days until all the non-transduced control cells were dead (approximately 7 days). The resulting cell populations were termed CalOB-Control for the negative control miRNA inhibitor cell line or CalOB- 219a for the *miR-219a-5p* miRNA inhibitor cell line; both were used for osteoblast differentiation assays as described above. The cells were then maintained in growth media supplemented with 0.5- μ g/mL puromycin. The puromycin was removed during the duration of the experiments to prevent any effects of the puromycin on cell function.

Alkaline phosphatase stain

The alkaline phosphatase enzymatic activity stain was performed using the Leukocyte Alkaline Phosphatase Kit (Sigma-Aldrich), which was modified to perform in tissue culture plates. Briefly, wells containing 7-day differentiated cells were washed twice in $1 \times$ phosphate-buffered saline (PBS), fixed in 3.75% paraformaldehyde (v/v in distilled water) for 15 min on ice, washed three times in $1 \times$ PBS, and allowed to dry completely. In a separate tube, 500 μ L of 100mM sodium nitrite solution were mixed with 500 μ L of 400mM FRV-alkaline solution (fast red violet LB base; v/v in hydrochloric acid) and allowed to stand for 2 min at room temperature. The solution was diluted 1:10 with double-distilled

water, and 500 μ L of naphthol AS-BI solution (naphthol AS-BI phosphate; 4 mg/mL in 2M 2-amino-2-methyl-1,3-propanediol [AMPD] buffer, pH 9.5) were added. One mL of the mixed solution was added to each well and allowed to incubate for 30 min in the dark. The plates were gently rinsed with distilled water, dried, and scanned.

Transfection of miRNA mimics and siRNAs

The *miR-219a-5p* (Catalog #MSY0000664; 5'-UGAUUGUCCAAACGCAAUUCU-3'), *miR-135a-5p* (Catalog #MSY0000147; 5'-UAUGGCUUUUUAUCCUAUGUGA-3'), and negative control (Catalog #YM00479902; 5'-UCACCGGGUGUAAAUCAGCUUG-3') double-stranded miRNA mimics were purchased from Qiagen. For the experiment illustrated in Fig. 3E, the miRNA mimics were transfected into primary mouse CalOBs using the 4D-Nucleofector (Lonza, Basel, Switzerland) according to the manufacturer's instructions. Specifically, 1×10^6 cells at approximately 70% confluence were trypsinized and transfected with 100nM of either mimic ($n = 6$) and plated into a 12-well plate. Cells were harvested in QIAzol (Qiagen) at either 6 or 24 hours following transfection for Ror β expression analysis. For the experiment illustrated in Fig. 5, 20nM negative control or *miR-219a-5p* mimic ($n = 6$) were transfected using HiPerFect Transfection Reagent (Qiagen) according to the manufacturer's instructions. The next day, the media were replaced with osteogenic differentiation media and cultured for 7 days (changing the media at days 3 and 6), where they were harvested in QIAzol. For the siRNA experiment illustrated in Fig. 6B to D, 20nM control or Ror β -specific siRNAs (Dharmacon, Lafayette, CO, USA; $n = 6$) were transfected using HiPerFect Transfection Reagent; the cells were cultured and harvested exactly as for the miRNA mimic experiments.

Ror β -3'UTR luciferase report construct and assay

To construct the 3'UTR reporter vector, the luciferase reporter gene *luc2P* was excised from the pGL4.11[*luc2P*] vector (Promega, Madison, WI, USA) as a HindIII/XbaI fragment. The *luc2P* reporter gene was used because it contains a C-terminal hPEST domain, a protein destabilization sequence, which allows for quicker and greater magnitude responses. The *luc2P* fragment was subcloned into the HindIII/XbaI sites of pcDNA/4TO (Promega) to make the 3'UTR reporter vector, Luc2P-4TO. The entire mouse Ror β 3'UTR sequence (7279 nucleotide bases in length; Genbank Accession NM_001043354), was synthesized as four approximately equal-sized gBLOCKs (Integrated DNA Technologies, Coralville, IA, USA) and assembled into the XbaI site of Luc2P-4TO using Gibson Assembly Master Mix (New England BioLabs, Ipswich, MA, USA) to produce Ror β -3'UTR-Luc. To assess the effects of *miR-219a-5p* on the Ror β 3'UTR, 100 ng of Ror β -3'UTR-Luc were cotransfected with 100nM of either negative control or *miR-219a-5p* miRNA mimics (Qiagen) into primary mouse CalOBs ($n = 6$) at approximately 70% confluence using DharmaFECT DUO transfection reagent (Dharmacon), a reagent specifically made for cotransfection of DNA and miRNAs. Twenty-four hours later, protein and luciferase assays were performed as previously described.⁽²⁶⁾ The data are presented as luciferase activity per μ g protein and normalized to the negative control miRNA mimic.

miRNA/mRNA pulldown assays

The miRNA pulldown assay was modified from Phatak and Donahue.⁽²⁷⁾ Briefly, custom miRIDIAN 3'-end biotinylated (*) double-stranded miRNA mimics for *mmu-miR-219a-5p* (5'-UGAUUGUCCAAACGCAAUUCU-3'*) and the same negative control miRNA sequence (Dharmacon), as described in the Transfection of miRNA mimics and siRNAs subsection (5'-UCACCGGGUGUAAAUCAGCUUG-3'*), were prepared. One million cells at approximately 70% confluence were trypsinized and transfected, using the 4D-Nucleofector (Lonza), with 100nM of either of the biotinylated mimics ($n = 3$) for 6 hours. Fifty μL of streptavidin-dyna beads (M-280; ThermoFisher Scientific) were sequentially washed twice using a tube magnet with solution A (0.1M NaOH [w/v] and 0.05M [w/v] NaCl in nuclease-free double-distilled water [ddH₂O]), twice with solution B (0.1M NaCl [w/v] and 70% ethanol [v/v] in ddH₂O) and three times with lysis buffer (20mM Tris-HCl [pH 7.5] [w/v], 100mM KCl [w/v], 5mM MgCl₂ [w/v], and 0.3% IGEPAL [v/v] in ddH₂O). All chemicals were purchased from Sigma-Aldrich unless otherwise stated. The beads were then pretreated with 10- μL yeast tRNA (10 mg/mL; ThermoFisher Scientific) in lysis buffer for 2 hours at 4°C and washed once with lysis buffer. Following the 6-hour transfection procedure, the cells were washed twice in ice-cold 1 \times PBS and lysed in 550 μL of lysis buffer (supplemented with Halt Protease Inhibitor and Riboblock RNase Inhibitor, both from Thermo-Fisher Scientific). Following a 10-min lysis on ice, the samples were centrifuged at 14,000 rpm and the supernatant saved. Fifty μL of each sample were saved as an “input” control; the remaining 500 μL were mixed with the prepared streptavidin beads overnight at 4°C. The bead-sample mixture was placed on the tube magnet and the beads washed three times with lysis buffer. The RNA was extracted by the addition of QIAzol (Qiagen). RNA isolation and cDNA synthesis were performed as described above on the whole RNA sample for the experimental pulldown, with 1 μg of the input control for each replicate. The data were calculated by first normalizing each pulldown to its own input control using $2^{\text{Input-Pulldown}}$. The three replicate samples for the *miR-219a-5p* and a negative control miRNA pulldowns were averaged and normalized to the negative control miRNA pulldown. These calculations gave enrichment values for the *miR-219a-5p* pulldown over the negative control miRNA pulldown.

Statistics

All values are expressed as mean \pm SEM. Mean values were compared between two groups and performed by an independent samples *t* test. Differences were considered significant at $p < 0.05$ (two-tailed test). For comparison among more than two groups, ANOVA was performed, followed by the Tukey's post hoc test, to adjust for multiple comparisons. Analyses were performed using the Statistical Package for the Social Sciences for Windows (Version 22.0; SPSS, Chicago, IL, USA); figures were created using GraphPad Prism (Version 5.03; GraphPad Software, San Diego, CA, USA).

Results

Identification of miRNAs predicted to regulate Ror β

miRNAs typically regulate gene expression through recognition and interaction with short seed sequences (typically seven to eight nucleotide bases) contained within the 3'UTRs of

their cognate target genes.^(10–12) Because both mouse and human *Rorβ* mRNAs contain relatively large 3'UTRs of approximately 7.3 kb and 7.6 kb, respectively (Fig. 1A, B), many miRNAs would be predicted to recognize the *Rorβ* 3'UTR with varying efficiencies. To reduce the list down to the most highly predicted miRNA/*Rorβ* mRNA interactions, we used the TargetScanMouse (Release 7.1; laboratory of David Bartel [Massachusetts Institute of Technology, Cambridge, MA, USA] in conjunction with the Whitehead Institute for Biomedical Research [Cambridge, MA, USA]) online prediction tool⁽²⁸⁾ to identify miRNAs that have the highest probability of conserved targeting (P_{CT} score).⁽²⁹⁾ We chose those nine miRNAs with the highest prediction scores (using a P_{CT} cutoff = 0.70) and ranked them separately in mice and humans (Fig. 1C). The predicted miRNA target sites were remarkably conserved between both species in terms of miRNA identity, number of miRNA binding sites, and location within the 3'UTR, suggesting a strong evolutionary conservation and regulatory function of *Rorβ* expression.

miRNA expression and activity in osteoblasts and aging

To begin to understand the regulatory function of these miRNAs with *Rorβ* expression and in osteoblast differentiation, we first conducted an osteoblast differentiation assay using WT primary murine CalOBs. The mRNA transcripts for *Alpl* (Supplemental Fig. 1A), *Bglap* (Supplemental Fig. 1B), *Coll1a1* (Supplemental Fig. 1C), and *Runx2* (Supplemental Fig. 1D) increased throughout the time course, demonstrating a normal osteoblast-differentiation gene-expression phenotype. As anticipated based on previous reports,⁽⁸⁾ *Rorβ* transcripts dramatically declined throughout the osteoblast differentiation time course (Fig. 2A). If any of these miRNAs do have a role in the regulation of *Rorβ* mRNA stability, which is one of the possible outcomes of miRNA-mediated silencing of gene expression,^(10,11) then the miRNA would be hypothesized to increase. Consistent with this hypothesis, *miR-219a-5p* (Fig. 2B), *miR-181a-5p* (Fig. 2D), *miR-218-5p* (Fig. 2E), *miR-135a-5p* (Fig. 2F), *miR-130a-3p* (Fig. 2G), *miR-148a-3p* (Fig. 2H), and *miR-199a-5p* (Fig. 2I) significantly increase to varying levels throughout the time course (compared with day 0), whereas *miR-125a-5p* expression (Fig. 2C) was unchanged and *miR-144-3p* was not expressed in CalOBs (data not shown). Remarkably, these data indicate that seven of the nine (78%) highest predicted miRNAs for *Rorβ* targeting follow a pattern consistent with *Rorβ* expression during osteoblast differentiation (eg, miRNA expression increased and *Rorβ* expression decreased).

To further refine the number of possible miRNAs that may be involved in the regulation of *Rorβ* levels, we took advantage of the fact that *Rorβ* expression dramatically increases in the bone cortex (containing mostly osteocytes and osteoblasts) during aging in both mice⁽⁹⁾ and humans.⁽⁷⁾ Following the same logic as in Fig. 2, if these miRNAs have a role in the regulation of *Rorβ* levels during aging, then they would be hypothesized to decrease in aged bone samples. Therefore, we profiled all nine of the miRNAs in young (6-month-old) and old (24-month-old) male mice, along with *Rorβ* expression. Although *Rorβ* levels in bone samples increased approximately 14-fold with age (Fig. 3A), only *miR-219a-5p* and *miR-135a-5p* decreased in old mice (Fig. 3B). Similarly, in primary bone core samples isolated from younger premenopausal women (mean age 27 years) and older postmenopausal women (mean age 78 years), where *Rorβ* levels increased ~1.6-fold (Fig.

3C), again only *miR-219a-5p* and *miR-135a-5p* decreased significantly in aging bone (Fig. 3D). The striking congruency of the downregulation of *miR-219a-5p* and *miR-135a-5p* expression in aging bone in both humans and mice, where *Rorβ* expression is increased, strongly suggests that these two miRNAs regulate *Rorβ* expression in bone. Indeed, transient transfection of synthetic *miR-219a-5p* and *miR-135a-5p* miRNA mimics into CalOBs resulted in significant suppression of *Rorβ* mRNA expression after 6 and 24 hours following transfection (Fig. 3E). It is important to note that although *miR-135a-5p* expression also inversely correlated with *Rorβ* expression during osteoblast differentiation and in aging bone, we chose to focus the next set of experiments on *miR-219a-5p* because it was the top predicted miRNA that regulates *Rorβ* in both mice and humans.

To assess the activity of *miR-219a-5p* in *Rorβ* 3'UTR regulation, we utilized a reporter assay where the 3'UTR of *Rorβ* was inserted 3' of a luciferase reporter gene (Fig. 4A). In this assay (Fig. 4B), if the cotransfected miRNA mimic regulates the 3'UTR and causes mRNA degradation and/or translational repression, then luciferase activity should decline. Indeed, cotransfection of the *Rorβ* 3'UTR reporter construct with *miR-219a-5p* miRNA mimic resulted in a significant suppression of luciferase activity (Fig. 4C).

***MiR-219a-5p* enhances osteoblastic differentiation**

We continued our analysis of *miR-219a-5p* and *Rorβ* regulation by determining whether transfection of a *miR-219a-5p* mimic into WT CalOB cells enhances osteoblast activity. CalOBs were transfected with either a negative control miRNA mimic or a *miR219a-5p* mimic, where *Rorβ* mRNA levels decreased by approximately 60% (Fig. 5A). The cells were then cultured in osteogenic differentiation medium for 7 days, where the *miR-219a-5p* mimic increased *Alpl* mRNA levels by 4.3-fold (Fig. 5B) and increased alkaline phosphatase staining (Fig. 5C).

We then performed the converse experiment, where either a negative control miRNA inhibitor or a *miR-219a-5p* inhibitor was introduced into WT CalOBs, producing the CalOB-Control or CalOB- 219a cell lines, respectively. As shown in Fig. 6A, *miR219a-5p* expression was significantly decreased by 95% in the CalOB- 219a cell model when compared with CalOB-Control cells, whereas *Rorβ* mRNA levels significantly increased by 3.4-fold (Fig. 6B, green bars). Additionally, *Alpl* mRNA expression was decreased by 77% (Fig. 6C, green bars) and alkaline phosphatase enzymatic activity was also noticeably decreased in the CalOB- 219a cell model as compared with CalOB-Control cells (Fig. 6D). To determine whether increased *Rorβ* levels in CalOB- 219a cells contribute to the suppressed osteogenic phenotype, control or *Rorβ*-specific siRNAs were transfected into CalOB- 219a cells. *Rorβ* mRNA levels decreased by 60% with the *Rorβ* specific siRNA (Fig. 6B, orange bars) and *Alpl* mRNA levels increased significantly (Fig. 6C, orange bars), relative to the control siRNA. The alkaline phosphatase staining in these conditions confirmed these observations (Fig. 6D). It should be noted that *Alpl* expression was not rescued to the same levels as observed in CalOB-Control cells, suggesting that factors other than *Rorβ* also contribute to the CalOB- 219a osteoblastic phenotype. Taken together, these results demonstrate that inhibition of *miR-219a-5p* suppresses the osteogenic phenotype, which is partially based on increased *Rorβ*.

Interaction of *miR-219a-5p* with *Rorβ* mRNA in osteoblasts

Finally, to confirm that *miR-219a-5p* directly targets *Rorβ* mRNA through direct interaction, we conducted a miRNA/mRNA pulldown assay using a transfected biotinylated *miR-219a-5p* mimic or biotinylated negative control mimic into WT CalOBs, followed by qPCR for the presence of the *Rorβ* mRNA (Fig. 7A). As shown in Fig. 7B, pulldown with the biotinylated *miR-219a-5p* mimic resulted in a 17-fold enrichment of *Rorβ* mRNA over the biotinylated negative control miRNA mimic. This demonstrates that *Rorβ* mRNA is a bona fide target of *miR-219a-5p* in osteoblasts through direct physical interaction.

Discussion

The goal of this study was to identify potential miRNAs that regulate *Rorβ* levels, both in an in vitro osteoblastic cell model and in vivo in both mouse and human bone fractions during physiological aging. We found that *miR-219a-5p* fits these criteria, as its expression increased during osteoblastic differentiation and decreased in both mouse and human bone during aging, exhibiting a reciprocal pattern to *Rorβ* expression. Furthermore, a *miR-219a-5p* mimic decreased *Rorβ* expression and enhanced osteoblast differentiation, whereas a *miR-219a-5p* inhibitor increased *Rorβ* expression and suppressed osteoblast differentiation. These data suggest that *miR-219a-5p* is bone anabolic, partially through suppression of *Rorβ*. Finally, we demonstrate that *miR-219a-5p* and *Rorβ* mRNA physically interact using a RNA-based pulldown assay. Collectively, these data demonstrate that *miR-219a-5p* regulates *Rorβ* levels in osteoblasts and bone, and that *miR-219a-5p* could represent a novel tool to suppress *Rorβ* activity and promote bone anabolism in the context of age-related bone disorders, such as osteoporosis.

It is estimated that over 1500 distinct miRNAs exist in both mice and humans, which regulate expression of approximately 60% of all genes in nearly every tissue,^(10,29,30) including bone.^(13–18) MiRNAs exert their regulatory function by triggering mRNA degradation and/or translational repression through the recognition of short miRNA seed sequences contained within the 3'UTR of target genes.^(11,12) In general, genes with longer 3'UTRs are more likely to be regulated by miRNAs simply based on their size.⁽³¹⁾ For example, expression of the isoform of *Nurr1* with the longer 3'UTR is under more miRNA control than the shorter isoforms.⁽³²⁾ Therefore, it is not surprising that *Rorβ*, with its long 3'UTR lengths of approximately 7.3 kb and approximately 7.6 kb in mice and humans, respectively, would likely be highly controlled by miRNAs. Using the TargetScan miRNA site prediction software,⁽²⁸⁾ we showed that many miRNAs are predicted to target *Rorβ* with varying efficiencies in both mice and humans. Interestingly, the identity and approximate location of the highly predicted miRNAs between mice and humans are also well conserved, providing evolutionary evidence of the importance of miRNA-mediated regulation of *Rorβ* expression. Of these sets of potential *Rorβ*-regulating miRNAs, one particular miRNA, *miR-219a-5p*, not only displayed the highest P_{CT} score (0.99) of all miRNAs for *Rorβ* 3'UTR recognition, but also recognizes three independent seed sequences in the *Rorβ* 3'UTR. This lends credence to the notion that *miR-219a-5p* would be predicted to have a significant function in the regulation of *Rorβ* expression levels.

The regulation of *Rorβ* expression is an important aspect of osteoblast biology, as its expression naturally decreases during differentiation and its constitutive expression of *Rorβ* inhibits differentiation.⁽⁸⁾ Our data suggest that *miR-219a-5p*, as well as a number of other miRNAs (Fig. 2), might have involvement in the regulation of *Rorβ* mRNA levels during osteoblast differentiation, as they increase in expression while *Rorβ* decreases. These other miRNAs may work in concert with *miR-219a-5p* to achieve this expression pattern, resulting in a cumulative effect on *Rorβ* mRNA levels. However, the effects of these same miRNAs on *Rorβ* mRNA levels in bone may be quite different in the context of aging. Contrary to what we observed in differentiating osteoblasts, the expression of only *miR-219a-5p* and *miR-135a-5p* changed in a manner consistent with increased *Rorβ* mRNA levels (eg, decreased miRNA expression) in both mice and humans, suggesting that the complete array of miRNAs controlling *Rorβ* expression during osteoblast differentiation and in aging bone are different.

Only a few reports have examined *miR-219a-5p* function in other systems, which may provide clues to its function in bone. Chang and colleagues demonstrated that *miR-219a-5p* is involved in vestibular compensation and that the predicted targets of *miR-219a-5p* were related to the processes of intracellular signal transmission, calcium/phosphate signaling, and cell–extracellular matrix interactions,⁽³⁰⁾ processes also known to be involved in bone metabolism. Kocerha et al. showed that *miR-219a-5p* negatively regulates the physiological function of N-methyl-D-aspartate glutamate receptors in the brain, which regulates neurotransmission and synaptic plasticity by downregulation of calcium/calmodulin-dependent protein kinase II γ subunit⁽³³⁾ that also has an important regulatory function in endochondral bone growth.⁽³⁴⁾ Interestingly, Dugas and colleagues demonstrated that *miR-219a-5p* is required for normal oligodendrocyte differentiation in the brain and is an inhibitor of cellular proliferation.⁽³⁵⁾ Because we know that *Rorβ* inhibits osteoblast differentiation and increases cellular proliferation,⁽⁸⁾ it is possible that *miR-219a-5p* may play a similar role in osteoblasts by promoting osteoblast differentiation through the downregulation of *Rorβ* levels. This is supported by our data that demonstrate that *miR-219a-5p* plays an anabolic role in osteoblast differentiation. Based on these observations, we propose that one function of *miR-219a-5p* is to suppress *Rorβ* levels and therefore promote differentiation. The function of *miR-219a-5p* in the context of aging bone may be similar; however, further experimentation (eg, *miR-219a-5p* transgenic mouse models) would be needed to clarify this role in vivo.

A limitation of this study is that only *miR-219a-5p* function was tested in calvarial osteoblasts, and not *miR-135a-5p*. Granted that *miR-135a-5p* levels also increased during osteoblast differentiation and decreased during aging, we chose to focus on *miR-219a-5p* for the following reasons. First, *miR-219a-5p* was the top predicted *Rorβ*-regulating miRNA in both mice and humans, with a P_{CT} score of 0.99. Second, three independent seed sequences for *miR-219a-5p* exist in the *Rorβ* 3'UTR, where only one exists for *miR-135a-5p*. Therefore, we considered *miR-219a-5p* as the prime candidate for further study. However, this does not preclude the possibility that *miR-135a-5p* may also be involved in *Rorβ* regulation during differentiation and in aging, although future studies would be necessary to characterize its role and whether it functions in unison with *miR-219a-5p* in *Rorβ* regulation. Another limitation is that we were not able to examine

correlations between the expression of *miR-219a-5p* in aging mouse and human bone fractions, as we did not obtain assessments of bone mass on these cohorts. Although bone loss in both mice and humans at these ages is well characterized,^(4,36) future studies would be needed to directly correlate *miR-219a-5p* expression with bone mass.

One of the most interesting aspects of this study is the striking congruency of *miR-219a-5p* expression during physiological aging in bone of both mice and humans. This is exemplified by the observation that Ror β levels increase in osteocyte-enriched bone fractions isolated both from mice^(8,9) and in bone core biopsies in humans⁽⁷⁾ during aging. Thus, Ror β and *miR-219a-5p* levels change similarly between mice and humans. Collectively, these findings strongly suggest that an identifiable Ror β /*miR-219a-5p* axis exists that is conserved in mammalian evolution. This opens up the possibility that clinical therapies involving the delivery of *miR-219a-5p* to osteoblast lineage cells in the context of human aging, where Ror β levels are high and promote bone catabolism,⁽⁸⁾ may be a useful approach in attenuating bone loss during aging.

Supplementary Material

Refer to Web version on PubMed Central for supplementary material.

Acknowledgments

This work was supported by NIH Grants R01 AR068275 (DGM), P01 AG004875 (SK/DGM), R01 AG048792 (SK/DGM), K01 AR070241 (JNF), K01 AR070281 (MMW), R01 AR049069 (AJV), and career development awards (JNF, MMW) from the Mayo Clinic Robert and Arlene Kogod Center on Aging. We would like to thank Mr. James Peterson for data analysis and Drs. John Hawse and Malayannan Subramaniam (Mayo Clinic) for the primary CalOBs used in this study.

References

1. Almeida M, O'Brien CA. Basic biology of skeletal aging: role of stress response pathways. *J Gerontol A Biol Sci Med Sci*. 2013;68(10): 1197–208. [PubMed: 23825036]
2. Bonewald LF. The amazing osteocyte. *J Bone Miner Res*. 2011;26(2): 229–38. [PubMed: 21254230]
3. Jilka RL, O'Brien CA. The role of osteocytes in age-related bone loss. *Curr Osteoporos Rep*. 2016;14(1):16–25. [PubMed: 26909563]
4. Khosla S Pathogenesis of age-related bone loss in humans. *J Gerontol A Biol Sci Med Sci*. 2013;68(10):1226–35. [PubMed: 22923429]
5. Wright NC, Looker AC, Saag KG, et al. The recent prevalence of osteoporosis and low bone mass in the United States based on bone mineral density at the femoral neck or lumbar spine. *J Bone Miner Res*. 2014;29(11):2520–6. [PubMed: 24771492]
6. Long F Building strong bones: molecular regulation of the osteoblast lineage. *Nat Rev Mol Cell Biol*. 2011;13(1):27–38. [PubMed: 22189423]
7. Roforth MM, Khosla S, Monroe DG. Identification of Ror β targets in cultured osteoblasts and in human bone. *Biochem Biophys Res Comm*. 2013;440(4):768–73. [PubMed: 24125721]
8. Roforth MM, Liu G, Khosla S, Monroe DG. Examination of nuclear receptor expression in osteoblasts reveals Ror β as an important regulator of osteogenesis. *J Bone Miner Res*. 2012;27:891–901. [PubMed: 22189870]
9. Farr JN, Weivoda MM, Nicks KM, et al. Osteoprotection through the deletion of the transcription factor Ror β in mice. *J Bone Miner Res*. 2018;33(4):720–31. [PubMed: 29206307]
10. Bartel DP. MicroRNAs: genomics, biogenesis, mechanism, and function. *Cell*. 2004;116(2):281–97. [PubMed: 14744438]

11. Kim VN, Nam JW. Genomics of microRNA. *Trends Genet.* 2006;22(3): 165–73. [PubMed: 16446010]
12. Bartel DP. MicroRNAs: target recognition and regulatory functions. *Cell.* 2009;136(2):215–33. [PubMed: 19167326]
13. He X, Eberhart JK, Postlethwait JH. MicroRNAs and micromanaging the skeleton in disease, development and evolution. *J Cell Mol Med.* 2009;13(4):606–18. [PubMed: 19220576]
14. Kobayashi T, Lu J, Cobb BS, et al. Dicer-dependent pathways regulate chondrocyte proliferation and differentiation. *Proc Natl Acad Sci U S A.* 2008;105(6):1949–54. [PubMed: 18238902]
15. Kronenberg HM. PTHrP and skeletal development. *Ann N Y Acad Sci.* 2006;1068:1–13. [PubMed: 16831900]
16. Gaur T, Hussain S, Mudhasani R, et al. Dicer inactivation in osteoprogenitor cells compromises fetal survival and bone formation, while excision in differentiated osteoblasts increases bone mass in the adult mouse. *Dev Biol.* 2010;340(1):10–21. [PubMed: 20079730]
17. Zhang Y, Xie RL, Gordon J, et al. Control of mesenchymal lineage progression by microRNAs targeting skeletal gene regulators *Trps1* and *Runx2*. *J Bio Chem.* 2012;287(26):21926–35. [PubMed: 22544738]
18. Davis C, Dukes A, Drewry M, et al. MicroRNA-183–5p increases with age in bone-derived extracellular vesicles, suppresses bone marrow stromal (stem) cell proliferation, and induces stem cell senescence. *Tissue Eng Part A.* 2017;23(21–22):1231–40. [PubMed: 28363268]
19. Dole NS, Delany AM. MicroRNA variants as genetic determinants of bone mass. *Bone.* 2016;84:57–68. [PubMed: 26723575]
20. Lian JB, Stein GS, van Wijnen AJ, et al. MicroRNA control of bone formation and homeostasis. *Nat Rev Endocrinol.* 2012;8(4): 212–27. [PubMed: 22290358]
21. Fujita K, Xing Q, Khosla S, Monroe DG. Mutual enhancement of differentiation of osteoblasts and osteocytes occurs through direct cell–cell contact. *J Cell Biochem.* 2014;115(11):2039–44. [PubMed: 25043105]
22. Farr JN, Roforth MM, Fujita K, et al. Effects of age and estrogen on skeletal gene expression in humans as assessed by RNA sequencing. *PLoS One.* 2015;10:e0138347. [PubMed: 26402159]
23. Modder UI, Oursler MJ, Khosla S, Monroe DG. *Wnt10b* activates the Wnt, notch, and *NFkappaB* pathways in U2OS osteosarcoma cells. *J Cell Biochem.* 2011;112(5):1392–402. [PubMed: 21321991]
24. Farr JN, Fraser DG, Wang H, et al. Identification of senescent cells in the bone microenvironment. *J Bone Miner Res.* 2016;31(11): 1920–9. [PubMed: 27341653]
25. Fujita K, Roforth MM, Demaray S, et al. Effects of estrogen on bone mRNA levels of sclerostin and other genes relevant to bone metabolism in postmenopausal women. *J Clin Endocrinol Metab.* 2014;99:E81–8. [PubMed: 24170101]
26. Modder UI, Rudnik V, Liu G, Khosla S, Monroe DG. A DNA binding mutation in estrogen receptor- α leads to suppression of Wnt signaling via *b-catenin* destabilization in osteoblasts. *J Cell Biochem.* 2012;113(7):2248–55. [PubMed: 22573547]
27. Phatak P, Donahue JM. Biotinylated micro-RNA pull down assay for identifying miRNA targets. *Bio-protocol.* 2017;7(9):e2253.
28. Agarwal V, Bell GW, Nam JW, Bartel DP. Predicting effective microRNA target sites in mammalian mRNAs. *Elife.* 2015;4.
29. Friedman RC, Farh KK, Burge CB, Bartel DP. Most mammalian mRNAs are conserved targets of microRNAs. *Genome Res.* 2009;19(1): 92–105. [PubMed: 18955434]
30. Chang MY, Park S, Choi JJ, et al. MicroRNAs 218a-5p, 219a-5p, and 221–3p regulate vestibular compensation. *Sci Rep.* 2017;7(1): 8701. [PubMed: 28821887]
31. Cheng C, Bhardwaj N, Gerstein M. The relationship between the evolution of microRNA targets and the length of their UTRs. *BMC Genomics.* 2009;10:431. [PubMed: 19751524]
32. Pereira LA, Munita R, Gonzalez MP, Andres ME. Long 3'UTR of *Nurr1* mRNAs is targeted by miRNAs in mesencephalic dopamine neurons. *PLoS One.* 2017;12(11):e0188177. [PubMed: 29145474]

33. Kocerha J, Faghihi MA, Lopez-Toledano MA, et al. MicroRNA-219 modulates NMDA receptor-mediated neurobehavioral dysfunction. *Proc Natl Acad Sci U S A*. 2009;106(9):3507–12. [PubMed: 19196972]
34. Li Y, Ahrens MJ, Wu A, Liu J, Dudley AT. Calcium/calmodulin-dependent protein kinase II activity regulates the proliferative potential of growth plate chondrocytes. *Development*. 2011;138(2):359–70. [PubMed: 21177348]
35. Dugas JC, Cuellar TL, Scholze A, et al. Dicer1 and miR-219 Are required for normal oligodendrocyte differentiation and myelination. *Neuron*. 2010;65(5):597–611. [PubMed: 20223197]
36. Glatt V, Canalis E, Stadmeier L, Bouxsein ML. Age-related changes in trabecular architecture differ in female and male C57BL/6J mice. *J Bone Miner Res*. 2007;22(8):1197–207. [PubMed: 17488199]

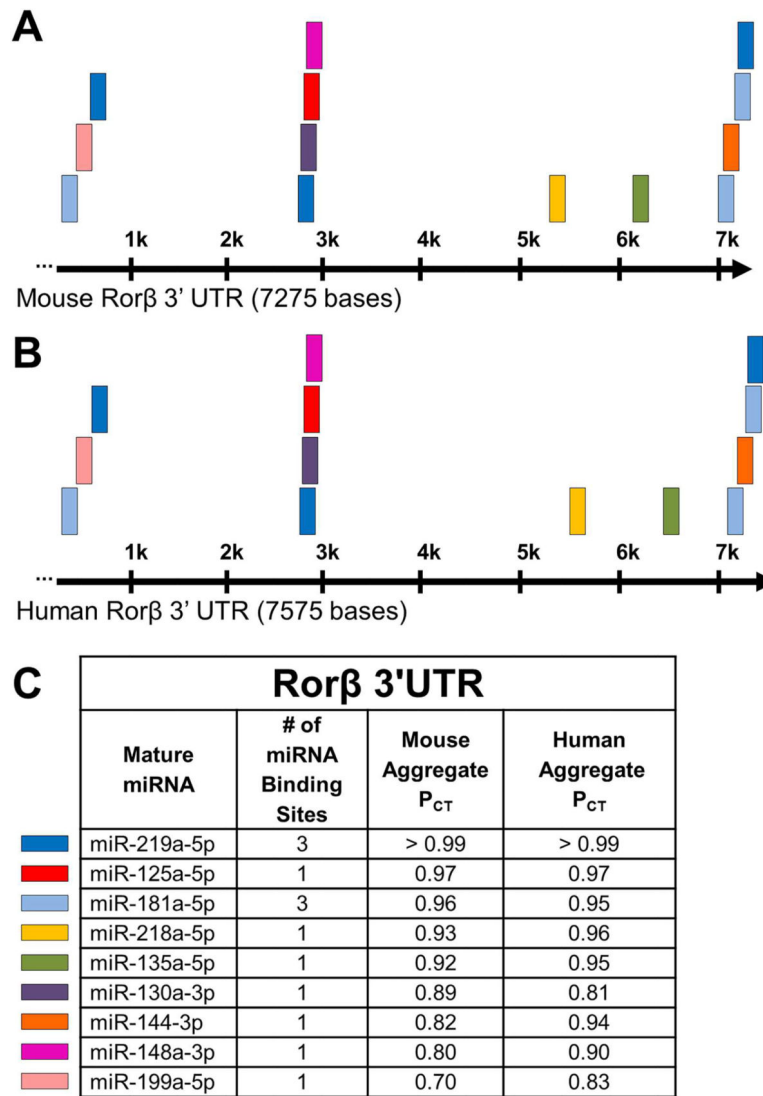
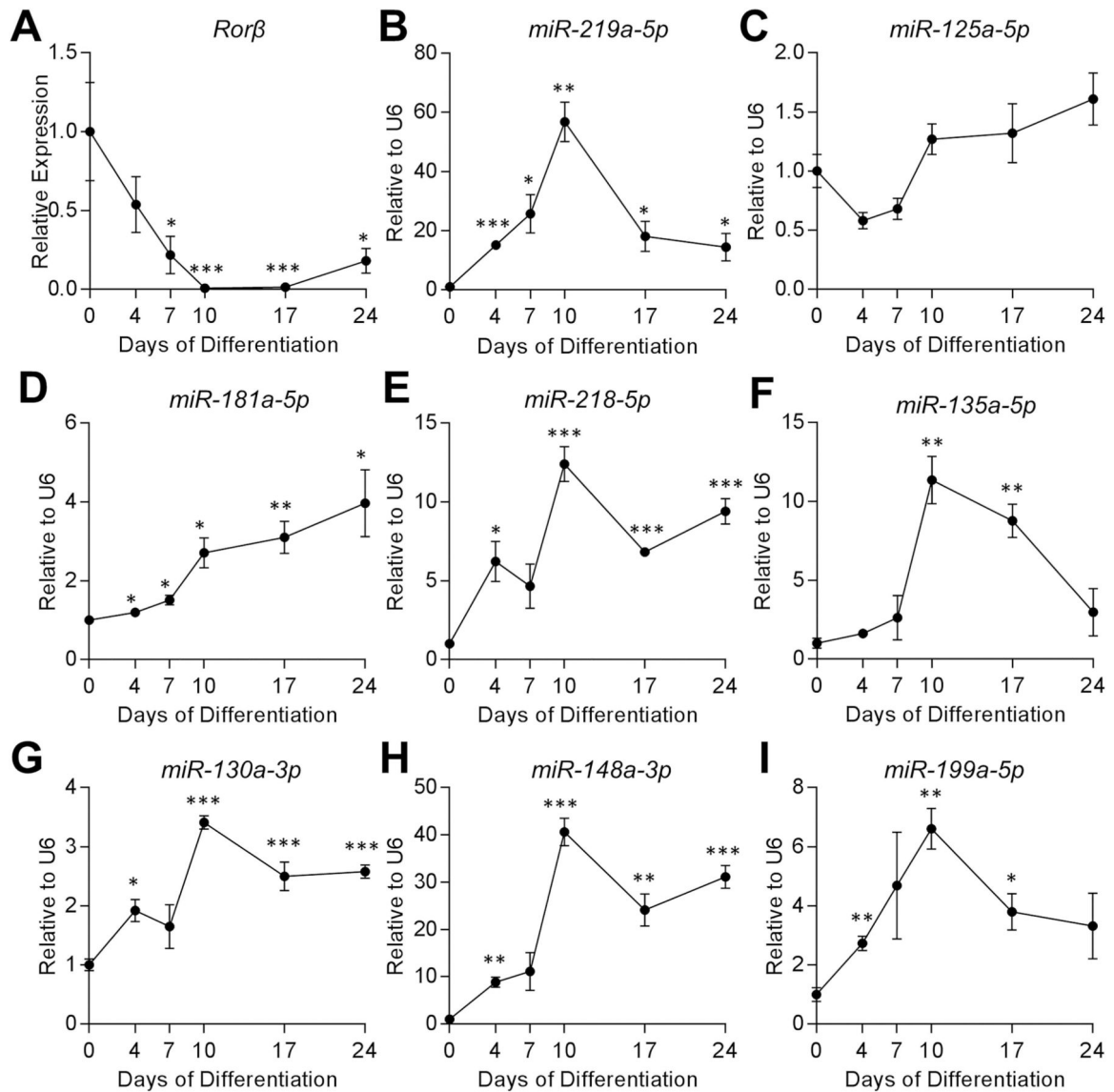


Fig. 1. Predicted miRNA target sites in the 3'UTR of mouse and human *Rorβ* mRNA. (A, B) Schematic representation of both mouse and human *Rorβ* 3'UTRs, with the length of each denoted in nucleotide bases. (C) Table of the top nine miRNAs with a P_{CT} score ≥ 0.70 against both mouse and human *Rorβ* mRNA 3'UTR. The mature miRNA name, number of binding sites, and the aggregate P_{CT} scores are listed. On the left of the table, color-coded boxes represent the location of each miRNA within the mouse and human *Rorβ* mRNA 3'UTR from the panels above.

**Fig. 2.**

Rorβ expression decreases, whereas expression of multiple miRNAs predicted to target *Rorβ* increases during osteoblastic differentiation. (A) Primary murine CalOBs were cultured in osteogenic differentiation medium and qPCR performed for *Rorβ* mRNA expression on samples collected at 0, 4, 7, 10, 17, and 24 days of differentiation ($n = 6$). (B–I) Similarly, expression analyses of the following miRNAs were also performed on the same osteoblast differentiation time course; (B) *miR-219a-5p*, (C) *miR-125a-5p*, (D) *miR-181a-5p*, (E) *miR-218-5p*, (F) *miR-135a-5p*, (G) *miR-130a-3p*, (H) *miR-148a-3p*, and (I) *miR-199a-5p*. Data represent mean \pm SEM. * $p < 0.05$; ** $p < 0.01$; *** $p < 0.001$ relative to day 0 (independent samples *t* test).

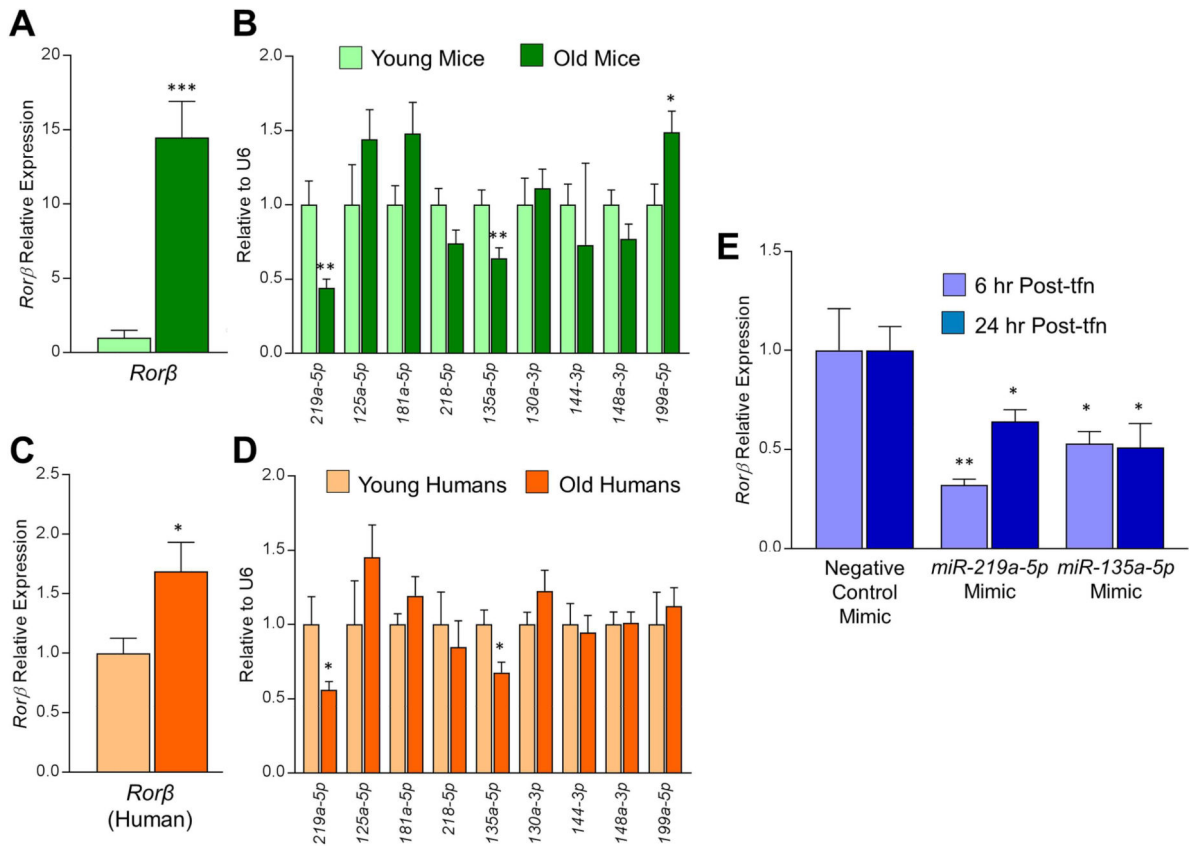


Fig. 3. *miR-219a-5p* and *miR-135a-5p* expression decline in aging bone in both mice and humans. (A, B) RNA was isolated from collagenase-digested vertebrae from either young (6-months-old) or old (24-months-old) male mice ($n = 10$) and subjected to qPCR analysis for: (A) *Rorβ* or (B) the panel of nine miRNAs predicted to regulate *Rorβ*. (C, D) Similarly, RNA isolated from needle biopsy bone core samples from younger (mean age 27 years) or older (mean age 78 years) women ($n = 10$) was also subjected to the same qPCR analysis for (C) *Rorβ* or (D) the same panel of nine miRNAs. (E) Synthetic miRNA mimics for *miR-219a-5p*, *miR-135a-5p*, or a negative control mimic were transfected into primary murine calvarial osteoblasts and RNA was isolated either 6 or 24 hours after transfection (Post-tfn) and qPCR analyses for *Rorβ* expression was performed. Data represent mean \pm SEM. * $p < 0.05$; ** $p < 0.01$; *** $p < 0.001$ relative to negative control mimic control transfection (independent samples t test).

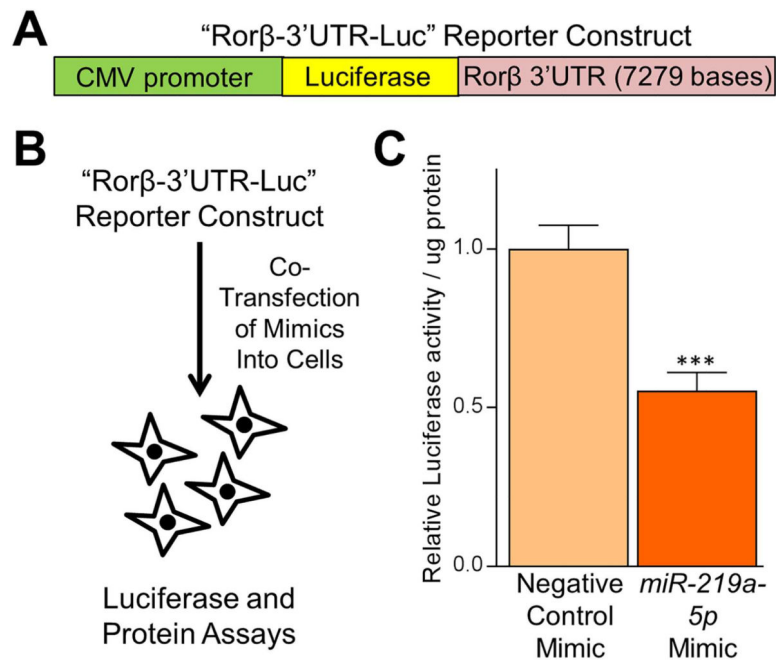


Fig. 4. A *miR-219a-5p* miRNA mimic regulates a Rorβ-3’UTR luciferase reporter construct. (A) Schematic diagram of the Rorβ-3’UTR-Luc reporter construct and (B) the miRNA/reporter assay in primary mouse CalOBs. (C) Relative luciferase activity per μg protein was measured 24 hours following cotransfection of the Rorβ-3’UTR-Luc reporter with either negative control or *miR-219a-5p* miRNA mimics. Data represent mean ± SEM. ****p* < 0.001 relative to negative control miRNA mimic (independent samples *t* test).

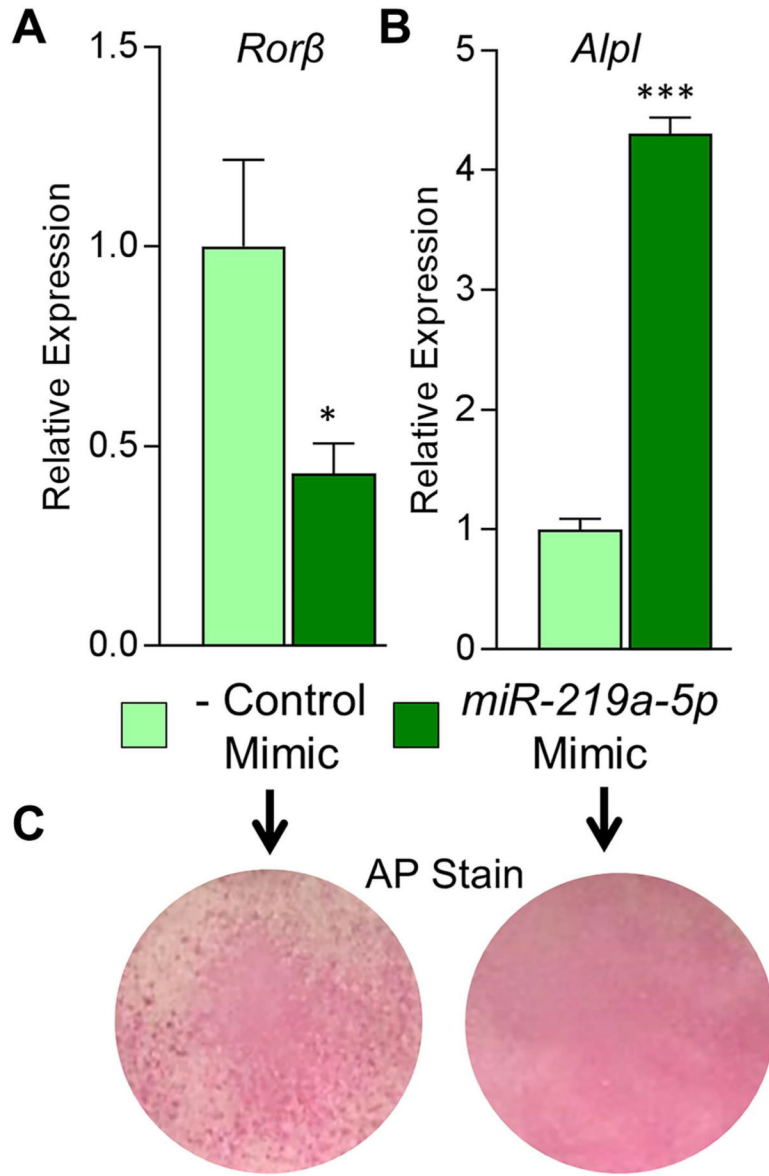


Fig. 5. A *miR-219a-5p* mimic enhances the osteogenic phenotype in osteoblasts. (A) Negative control (-) or *miR-219a-5p* miRNA mimics were transfected into CalOB cells and assayed for *Rorb* expression using qPCR. (B) The transfected cells were cultured in osteogenic differentiation medium for 7 days and *Alpl* expression assessed using qPCR. (C) Alkaline phosphatase enzymatic activity (AP stain) was assessed at 7 days of differentiation for both transfection conditions. Data represent mean \pm SEM. * $p < 0.05$; *** $p < 0.001$ relative to negative control miRNA mimic (independent samples *t* test).

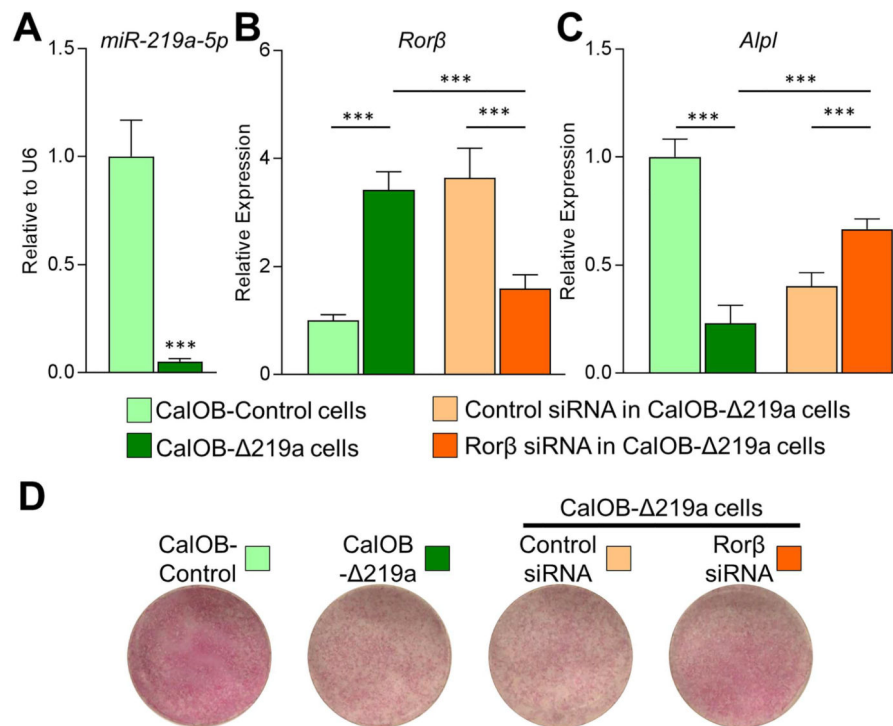


Fig. 6. A *miR-219a-5p* inhibitor suppresses the osteogenic phenotype in osteoblasts. Control murine calvarial osteoblasts (CalOB-Control) and CalOB- 219a cells were assayed for (A) *miR-219a-5p* and (B) *Rorβ* expression using qPCR. (C) CalOB and CalOB- 219a cells were cultured in osteogenic differentiation medium for 7 days and *Alpl* expression levels were assayed using qPCR (green bars). Control or *Rorβ*-specific siRNAs were transfected into CalOB- 219a cells, cultured in osteogenic differentiation medium for 7 days, and assayed for *Rorβ* or *Alpl* expression (panels B–C, orange bars). (D) Alkaline phosphatase enzymatic activity was assessed at 7 days of differentiation for the indicated conditions. Data represent mean \pm SEM. *** $p < 0.001$ (ANOVA followed by Tukey's post hoc test).

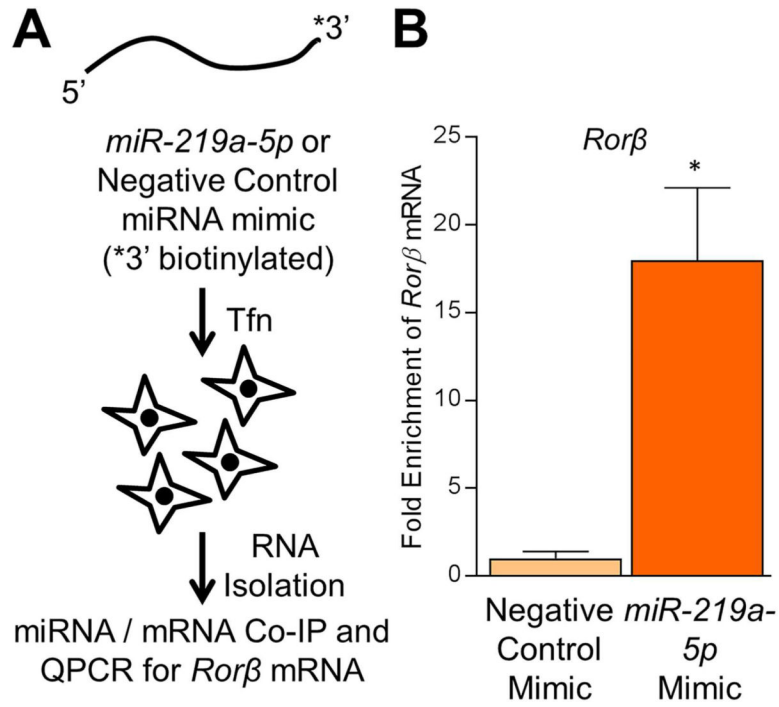


Fig. 7. *miR-219a-5p* interacts with *Rorβ* mRNA in osteoblasts. (A) Schematic diagram of the miRNA/mRNA pulldown assay used in this study. (B) Fold enrichment of *Rorβ* mRNA by the biotinylated *miR-219a-5p* mimic (over the biotinylated negative control mimic) was determined by qPCR. Data represent mean ± SEM. **p* < 0.05 relative to the negative control mimic (independent samples *t* test).